Tectonophysics, 140 (1987) 49–63
Elsevier Science Publishers B.V., Amsterdam – Printed in The Netherlands

The crustal structure of the axis of the Great Valley, California, from seismic refraction measurements

W. STEVEN HOLBROOK [1] and WALTER D. MOONEY [2]

[1] *Geophysics Department, Stanford University, Stanford, CA 94305 (U.S.A.)*
[2] *U.S. Geological Survey, MS 977, 345 Middlefield Road, Menlo Park, CA 94025 (U.S.A.)*

(Received March 18, 1986; accepted June 15, 1986)

Abstract

Holbrook, W.S. and Mooney, W.D., 1987. The crustal structure of the axis of the Great Valley, California, from seismic refraction measurements. In: S. Asano and W.D. Mooney (Editors), Seismic Studies of the Continental Lithosphere. *Tectonophysics*, 140: 49–63.

In 1982 the U.S. Geological Survey collected six seismic refraction profiles in the Great Valley of California: three axial profiles with a maximum shot-to-receiver offset of 160 km, and three shorter profiles perpendicular to the valley axis. This paper presents the results of two-dimensional raytracing and synthetic seismogram modeling of the central axial profile. The crust of the central Great Valley is laterally heterogeneous along its axis, but generally consists of a sedimentary section overlying distinct upper, middle, and lower crustal units. The sedimentary rocks are 3–5 km thick along the profile, with velocities increasing with depth from 1.6 to 4.0 km/s. The basement (upper crust) consists of four units: (1) a 1.0–1.5 km thick layer of velocity 5.4–5.8 km/s, (2) a 3–4 km thick layer of velocity 6.0–6.3 km/s, (3) a 1.5–3.0 km thick layer of velocity 6.5–6.6 km/s, and (4) a laterally discontinuous, 1.5 km thick layer of velocity 6.8–7.0 km/s. The mid-crust lies at 11–14 km depth, is 5–8 km thick, and has a velocity of 6.6–6.7 km/s. On the northwest side of our profile the mid-crust is a low-velocity zone beneath the 6.8–7.0 km/s lid. The lower crust lies at 16–19 km depth, is 7–13 km thick, and has a velocity of 6.9–7.2 km/s. Crustal thickness increases from 26 to 29 km from NW to SE in the model.

Although an unequivocal determination of crustal composition is not possible from P-wave velocities alone, our model has several geological and tectonic implications. We interpret the upper 7 km of basement on the northwest side of the profile as an ophiolitic fragment, since its thickness and velocity structure are consistent with that of oceanic crust. This fragment, which is not present 10–15 km to the west of the refraction profile, is probably at least partially responsible for the Great Valley gravity and magnetic anomalies, whose peaks lie about 10 km east of our profile. The middle and lower crust are probably gabbroic and the product of magmatic or tectonic underplating, or both. The crustal structure of the Great Valley is dissimilar to that of the adjacent Diablo Range, suggesting the existence of a fault or suture zone throughout the crust between these provinces.

Introduction

The Great Valley of California is a 700-km-long by 100-km-wide sedimentary basin situated between the granitic and metamorphic terrane of the Sierra Nevada and the Franciscan subduction complex of the Coast Ranges. The sedimentary rocks of the Great Valley, which include the late Jurassic to late Cretaceous age Great Valley Sequence and overlying Cenozoic units, form an asymmetric syncline with a steeply-dipping west limb and a gently-dipping east limb (e.g., Dickinson, 1981). The Great Valley is of geologic interest not only as a prolific oil-bearing province, but also as a key to the tectonic evolution of central California.

Recent geological work, most notably in the Coast Ranges (e.g., Blake et al., 1984) and Sierra

0040-1951/87/$03.50

Nevada (e.g., Day et al., 1985), has greatly improved our understanding of the Mesozoic and Cenozoic evolution of the California continental margin; still, many important questions remain unanswered. The outstanding problems include: (1) the composition of the basement beneath the

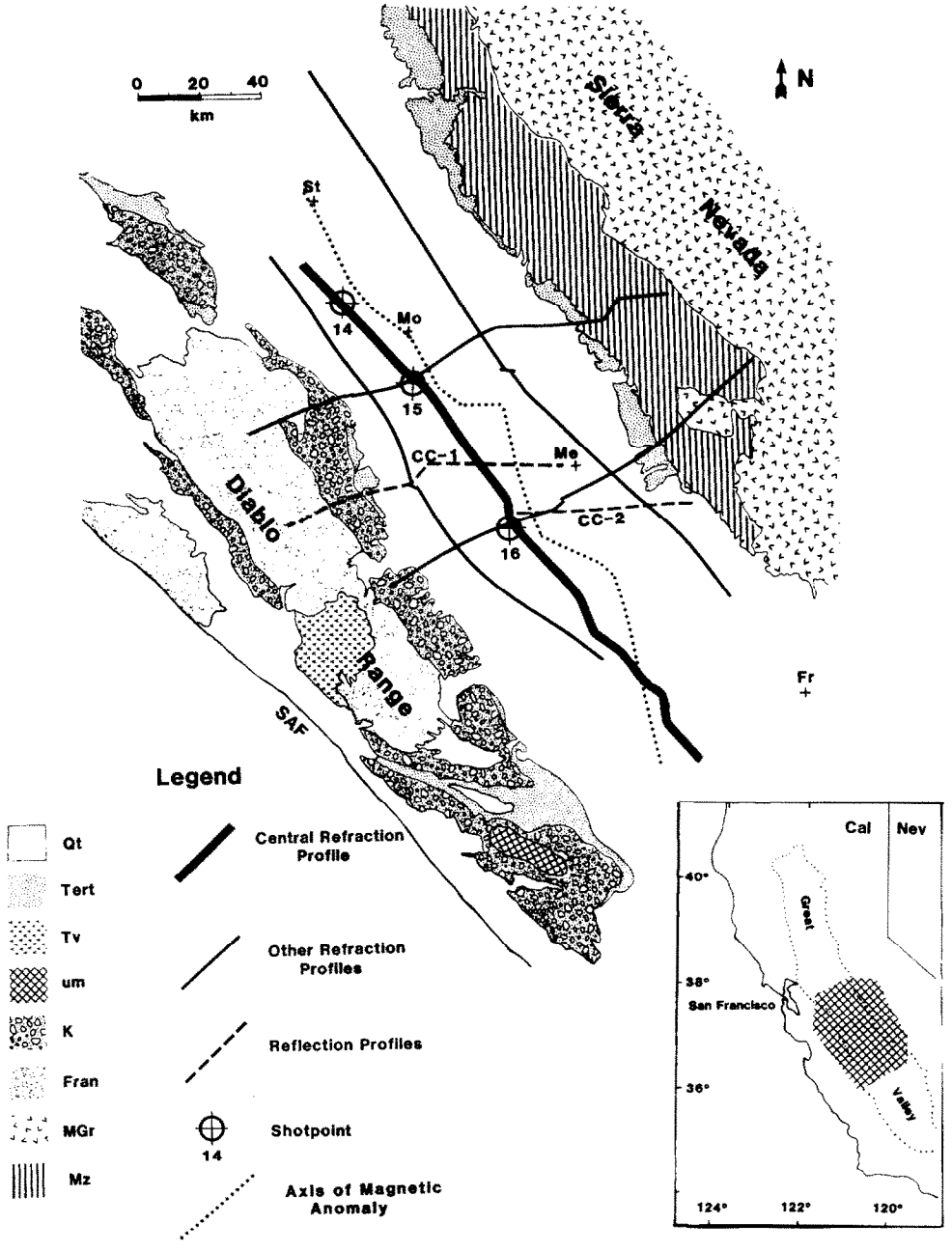

Fig. 1. Location map of Great Valley, California, showing refraction lines, reflection lines, generalized geology, and the approximate location of the peak of the Great Valley magnetic anomaly (Cady, 1975). *Qt* = Quaternary sediments; *Tert* = Tertiary sediments; *Tv* = Tertiary volcanics; *um* = ultramafics; *K* = Cretaceous sedimentary rocks, largely the Great Valley Sequence; *Fran* = Jurassic and Cretaceous Franciscan melange; *MGr* = Mesozoic granites and granodiorites of the Sierra Nevada; *Mz* = undifferentiated Mesozoic rocks, including Sierra greenstone belt. *SAF*—San Andreas Fault; *St*—Stockton; *Mo*—Modesto; *Me*—Merced; *Fr*—Fresno.

Great Valley, (2) the existence and location of the postulated contact between continental Sierra Nevada crust and oceanic-affinity crust further west, (3) the cause of the Great Valley magnetic and gravity anomalies (Cady, 1975; Griscom, 1982; Griscom and Jachens, 1986), (4) the relationship between the Coast Range Ophiolite and the Smartville Ophiolite of the western Sierra Nevada, and (5) the crustal thickness and composition of the deep crust of the Great Valley. Because the answers to these questions are concealed beneath the sediments of the Great Valley, geophysical methods must be used to investigate them.

In order to pursue these questions, the U.S. Geological Survey (USGS) conducted a seismic refraction survey in June, 1982, in the Great Valley between the latitudes of Stockton and Fresno (Fig. 1). The refraction survey, part of a larger seismic refraction and reflection program in the Great Valley, consisted of three axial lines, with a maximum shot-to-receiver offset of 165 km, and three shorter cross-lines perpendicular to the valley axis. This paper presents the results of an interpretation of the central axial refraction profile. We begin with a description of the data, present a model consistent with the observed seismic phases, then discuss some of the geological implications of that model.

Refraction data

The Great Valley central axial profile consists of three shotpoints (SP14, 15, and 16) along a 180 km-long line (Fig. 1). Seismic energy was generated by 800- to 1600-kg chemical explosions and recorded on FM analog tape by 120 portable seismographs (Healy et al., 1982). Final record sections were filtered 1–10 Hz and plotted in normalized (Fig. 2) and true amplitude format.

The refraction data provide information on the compressional-wave velocity and structure of the entire crust and uppermost mantle. The shot spacings of 30 km and 50 km provide good reversed control on the sedimentary and upper crustal velocities, but the velocities of the lower crust and upper mantle are unreversed. The observed phases are generally similar on the three shots, as would be expected on an axial line in a linear province such as the Great Valley. Figure 3 shows a generalized travel-time curve for the major phases observed on the three shots. Not all of these general phases are present on all profiles, however, indicating significant lateral variation along the axis of the valley. The following section describes the phases observed on the three shots.

Shotpoint 14

The maximum shot-receiver offset of SP14 is long enough (160 km) to record refracted and reflected arrivals from the entire crust and uppermost mantle. At near offset, first arrivals with apparent velocities of about 1.8 to 4.0 km/s (*A* and *B*, Fig. 4) represent energy refracted in the sedimentary section. Behind these arrivals a prominent basement reflection (*C*, Fig. 4) asymptotes to an apparent velocity of 4.0 km/s, which is inferred as the velocity at the base of the sedimentary section. Control on the velocity gradients within the sedimentary section comes from prominent multiple refractions (*AA*, Fig. 4) which arrive at twice the travel time and distance of first arrivals from the sediments and basement. Beyond 15 km, first arrivals refracted from three distinct upper crustal layers have apparent velocities of 6.3, 6.6, and 7.2 km/s (branches *E*, *F*, and *G*, Fig. 4); however, reversals from the other shotpoints indicate that these are all updip, i.e. higher-than-actual, velocities. At least two strong upper-crustal reflections arrive behind these upper-crustal refractions.

Arrivals from the deep crust and upper mantle yield apparent velocities of 7.0 (*I*, Fig. 4) and 8.1 km/s (*J*, Fig. 4), respectively, for these layers. These velocities are unreversed, since the maximum offset on SP16 is too short to record these phases (cf. Fig. 2). The Moho reflection (*I*, P_mP) is prominent beyond 75 km and is the highest-amplitude phase on true-amplitude records. Beyond 110 km, P_mP is immediately followed by high-amplitude, ringing arrivals which may be peg-leg multiples from within the crust or reflections from within the mantle, which we have not modeled. A delay of about 1.0 sec of P_mP (*I*) with respect to the extrapolation of the 7.2 km/s upper-crustal phase (*G*), combined with the rapid amplitude

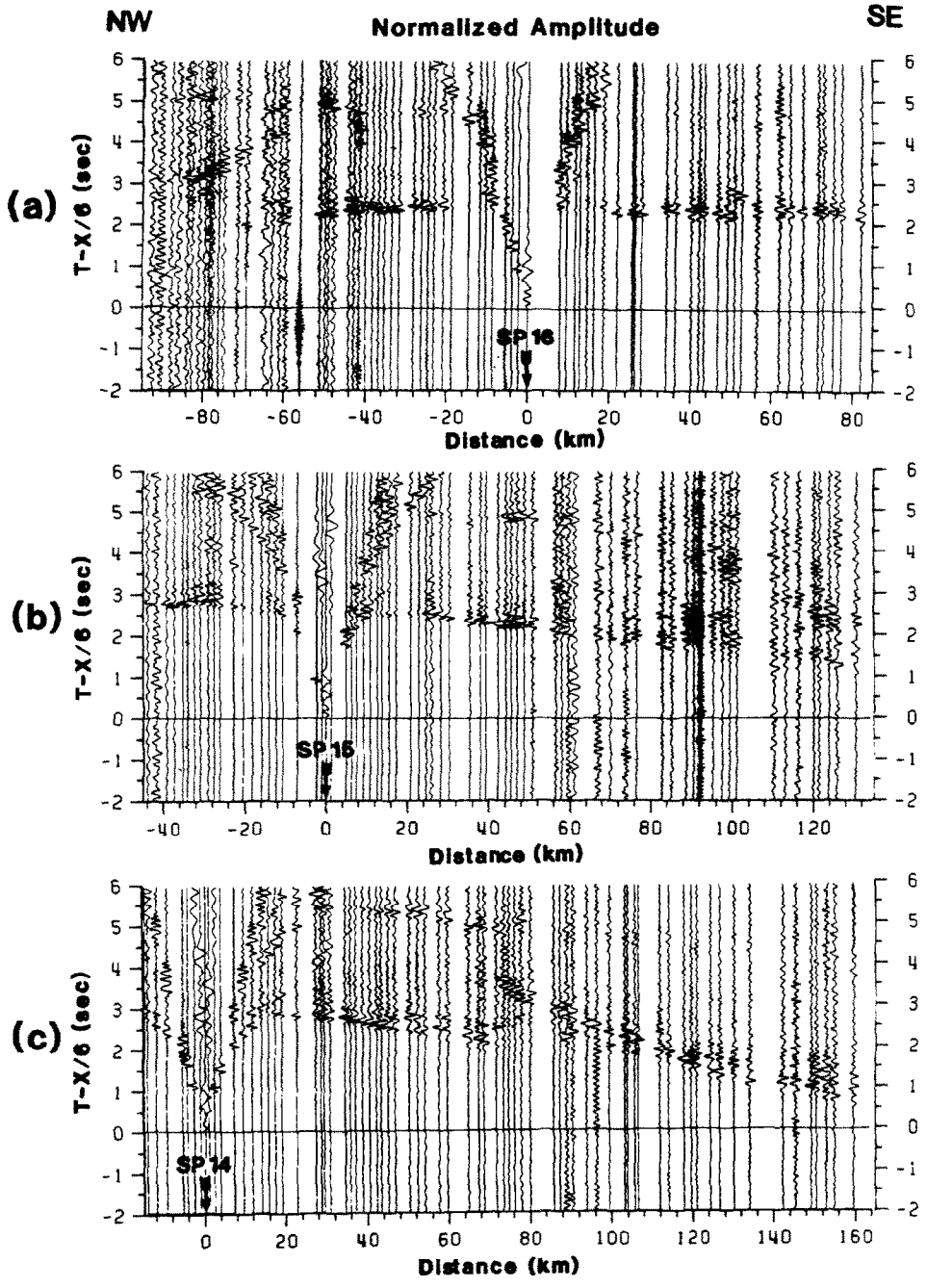

Fig. 2. Refraction data from central axial profile, plotted in trace-normalized format. (a) SP16, (b) SP15, (c) SP14.

decay of the 7.2 km/s phase beyond 80 km, indicates a velocity inversion in the mid-crust.

Shotpoint 15

The data from SP15 (Fig. 5) show most of the same phases observed on SP14. To the northwest, sediment velocities range from about 1.8 to 3.9 km/s. Beyond the crossover at 12 km, first arrivals from the topmost upper crustal layers have down-dip apparent velocities of 5.7 and 6.1 km/s (*E* and *F*, Fig. 5). To the southeast, sediment velocities range from about 1.8 to 3.8 km/s. Beyond the crossover to basement at 10 km, first arrivals from

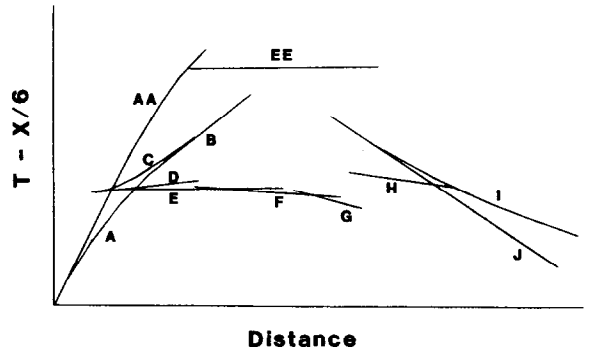

Fig. 3. Generalized traveltime curve for shots on central axial profile. *A*, *B*—arrivals from sediments of Great Valley; *C*—reflection from top of valley basement; *D*—refraction from basement "hidden layer"; *E*, *F*, *G*—refractions from upper-crustal layers; *H*—reflection from top of lower-crustal layer; *I*—reflection from crust–mantle boundary; *J*—refraction from uppermost mantle; *AA*—multiple arrival which refracts through sediments, reflects off surface, and refracts again through sediments; *EE*—superposition of basement refracted reflections, reflected refractions, and multiples.

the three upper crustal layers have updip apparent velocities of 6.1, 6.5, and 6.9 km/s (*E*, *F*, and *G*, Fig. 5). Prominent sedimentary (*AA*, Fig. 5) and basement (*EE*, Fig. 5) multiples are visible in both directions. P_mP can be traced with difficulty to the southeast from about 80 km through several strong pulses at 120 km. About 1.5 s behind P_mP are several ringing arrivals which may represent peg-leg multiples or reflections from within the upper mantle. The amplitude decay of phase *G* beyond 100 km again indicates a mid-crustal velocity inversion. However, the inversion is less pronounced than that determined further to the northwest, since on SP15 P_mP is delayed only 0.4 s with respect to the extrapolation of the 6.9 km/s upper crustal phase, while on SP14 P_mP is delayed a full second.

Shotpoint 16

The data from SP16 (Fig. 6) also show phases similar to those observed on SP14 and SP15. To the northwest, sediment velocities range from about 1.8 to 2.9 km/s. Beyond the crossover to basement at 8 km, first arrivals from the three upper crustal layers have downdip apparent velocities of 5.9, 6.3, and 6.8 km/s (*E*, *F*, and *G*, Fig. 6). To the southeast, the maximum sediment velocity is about 3.0 km/s. Beyond the crossover at 7 km, first arrivals from the topmost upper crustal layers have apparent velocities of 6.1 and 6.4 km/s. Unlike on SP14 and SP15, the third and fastest upper crustal refraction (*G*) is absent to the southeast. Sedimentary and basement multiples are again visible in both directions. P_mP is visible to the northwest beyond about 65 km; to the southeast P_mP is absent, indicating that the critical point for P_mP lies beyond 85 km in that direction. A high-amplitude reflection which appears beyond 50 km is probably from the top of a deep-crustal layer.

Modeling

The velocity model we derived (Fig. 7) is based primarily on iterative travel time modeling using 2-D raytracing (Červený et al., 1977). Velocities above and below interfaces are also constrained by the locations of critical points of reflections. Additional details of the model, such as velocity gradients within layers, are based on amplitude modeling using 2-D synthetic seismograms (McMechan and Mooney, 1980). Because the Great Valley is a remarkably two-dimensional feature—its gravity and magnetic anomalies are nearly continuous along much of its length—we tried, as much as possible, to minimize lateral variation along this axial model. Nevertheless, the data require significant lateral variation, perhaps in part because the azimuth of the northwest end of the profile is slightly oblique to the axis of the valley.

The velocities and structure of the valley sediments and upper crust are well-constrained by reversed arrivals from the three shots. The sedimentary section is modeled as three layers, each with a different, positive velocity gradient, in order to match the travel times and relative amplitudes of the primary (*A*) and multiple (*AA*) sedimentary arrivals. The thickness of the sediments, determined from drill-hole data over most of the profile (Bartow, 1983), increases from 3 km in the southeast to about 5 km in the northwest. The uppermost basement layer is modeled as a 1.0–1.5 km thick transition zone with a velocity of 5.5–5.7

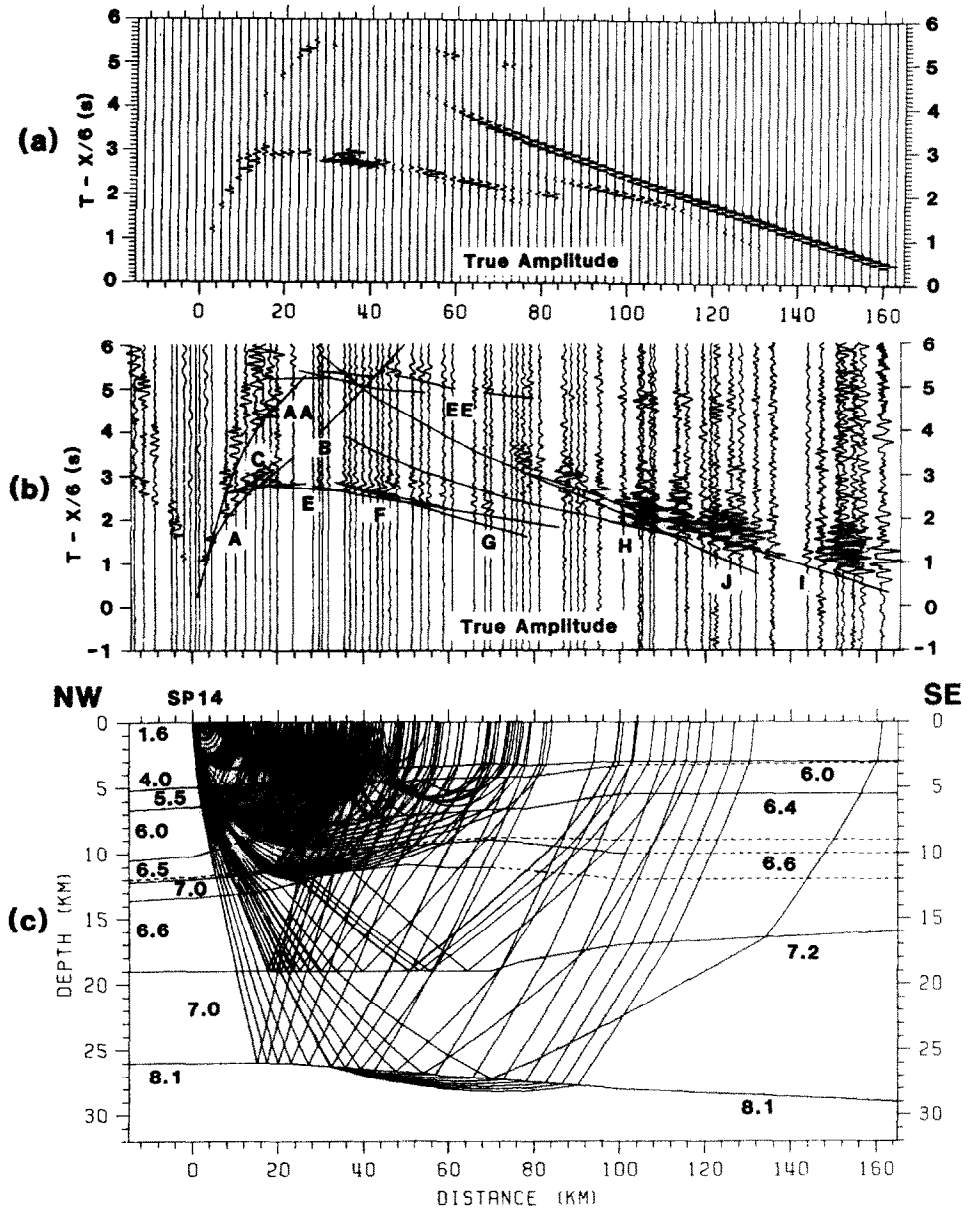

Fig. 4. Model for SP14. a. Two-dimensional synthetic seismogram, in true amplitude scaled by distance raised to the 1.5 power. Distance scale relative to shotpoint. b. True-amplitude data and calculated travel-time curves for model; nomenclature as in Fig. 3. c. Raytrace diagram for SP15. Distance scale relative to model.

km/s, based on the critical point of the basement reflection (*C*, Fig. 4). This uppermost basement layer is a seismological "hidden layer", that is, it is too thin to generate interpretable first arrivals but must be included if the model is to match drill-hole basement depths.

Beneath the hidden layer, the upper crust comprises three layers whose tops lie at depths of about 7, 10, and 12 km, and whose velocities are 6.0–6.3, 6.4–6.5, and 7.0 km/s, respectively. The northwestward component of dip of these layers in the profile is confirmed by the reversed first arrivals; the 7.0 km/s layer, for example, generates an updip apparent velocity of 7.2 km/s on SP14 (*G*, Fig. 4) and a downdip apparent velocity of 6.8 km/s on SP16 (*G*, Fig. 7). The strong

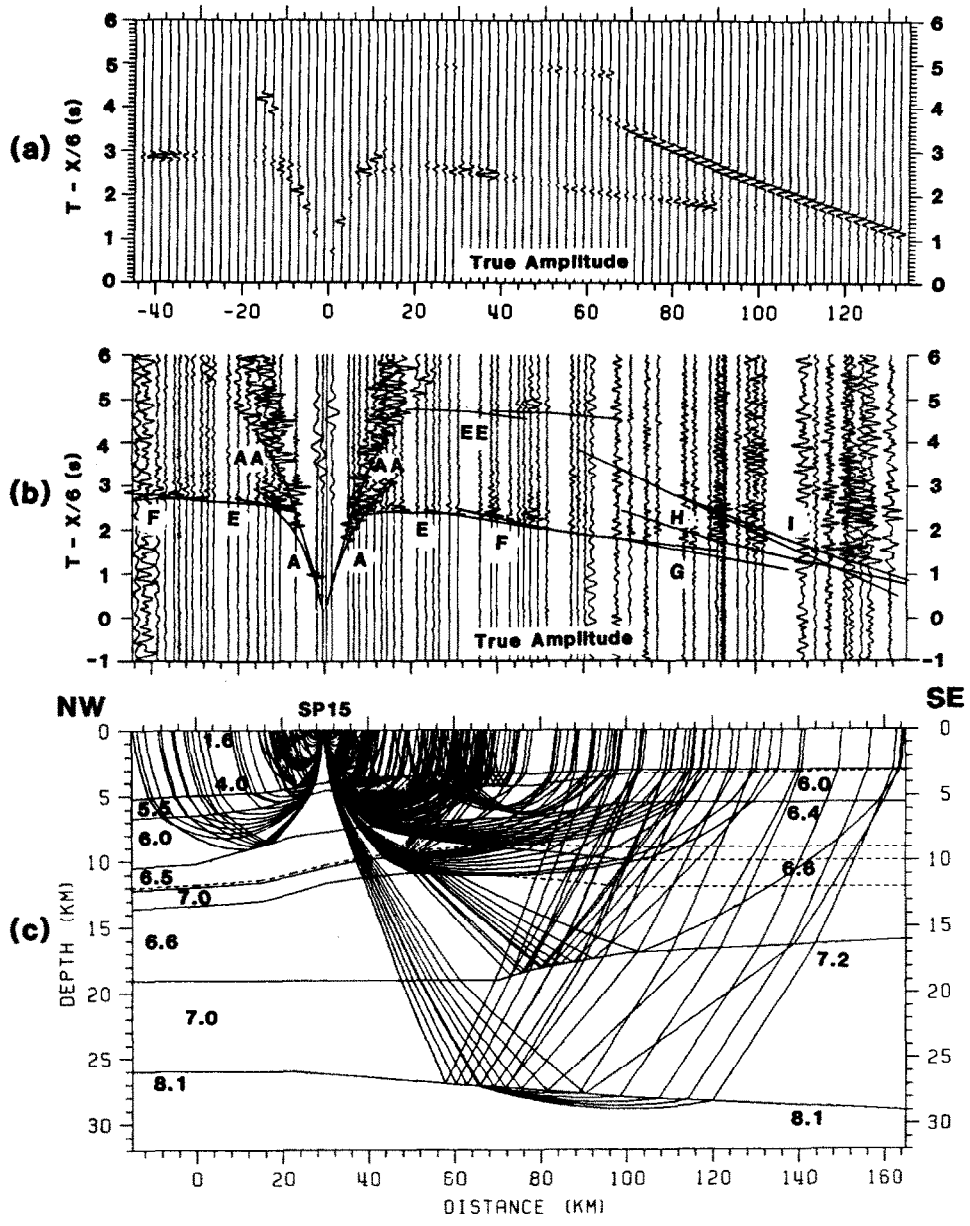

Fig. 5. Model for SP15. (a), (b), and (c) as in Fig. 4.

velocity gradient in the 6.0 km/s layer (from 6.0 to 6.3 km/s) is required to generate the strong amplitudes observed on the basement multiple (*EE*, Fig. 5). The 7.0 km/s layer, which has important geological implications, disappears southeast of SP15, where it is replaced by crust of velocity 6.5–6.6 km/s (*F–G*, Fig. 6).

An alternative model, in which the upper-crustal 7.0 km/s layer does not disappear to the southeast, cannot be ruled out by the seismic data. Because the southeastern half of the model is unreversed, it is possible that the slow apparent velocities (6.5–6.6 km/s) on SP15-southeast are the result of a relatively steep (about 5°–10°) southeasterly component of dip of the 7.0 km/s layer, rather than its replacement in the crust by slower material. This model is less attractive, however, for two reasons. First, the preferred model is more compatible with Bouguer gravity data: preliminary 2-D gravity modeling shows that the

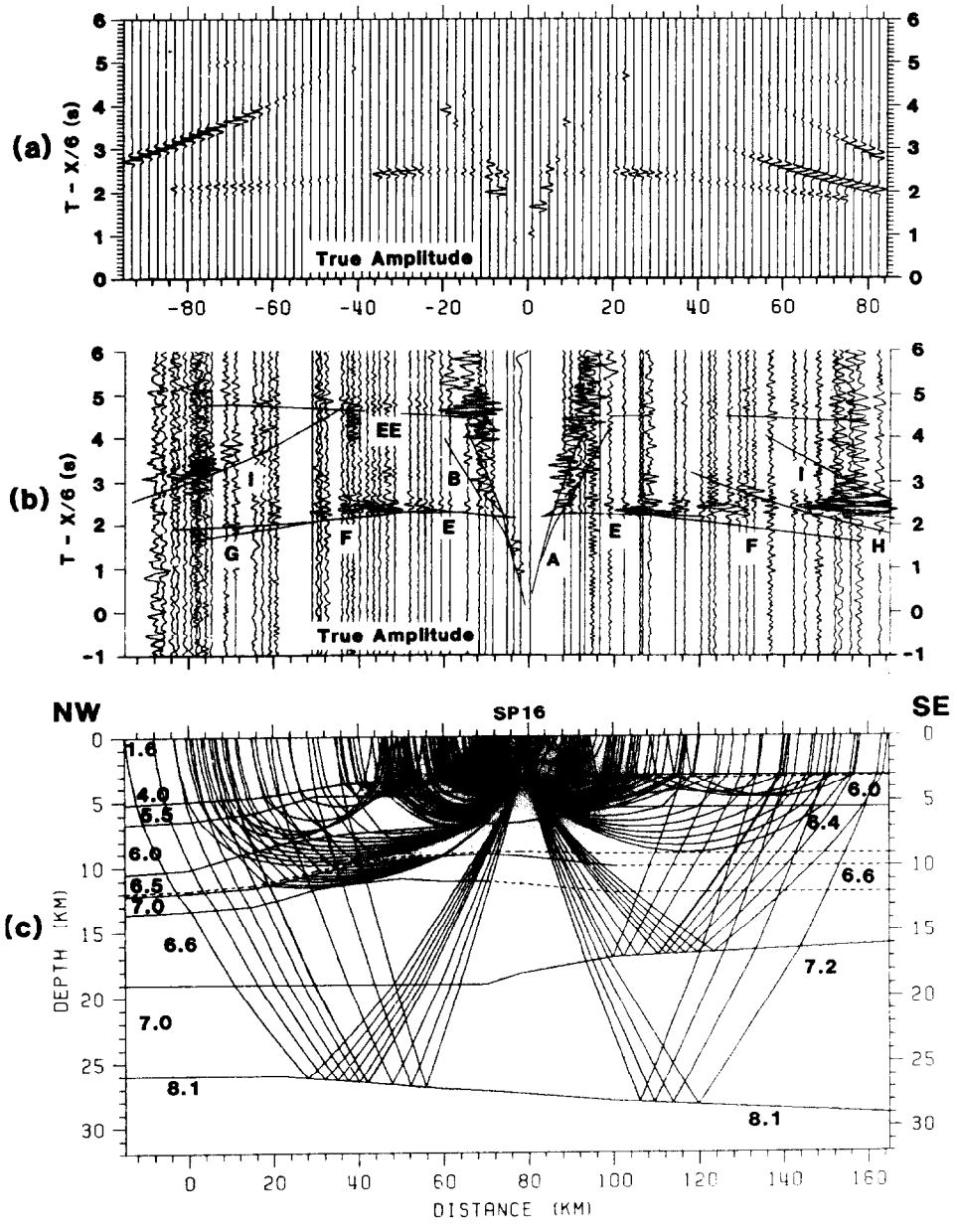

Fig. 6. Model for SP16. (a), (b), and (c) as in Fig. 4.

alternative model would create a gravity anomaly of about 50 mGal, much greater than the observed 10–15 mGal anomaly. Second, as discussed in greater detail below, the 7.0 km/s layer is not present beneath the refraction profile 15 km to the west (Colburn and Mooney, 1986); there is therefore little reason to expect it to be continuous for 180 km along the strike of the valley.

Although no true reversed refractions from the lower crust or upper mantle were recorded in this experiment, the deep velocity structure can be constrained by using the locations of critical points and the asymptotic apparent velocities of deep reflections. As previously described, a low-velocity layer (LVL) beneath the mid-crustal 7.0 km/s layer is most clearly indicated by the 1.0-s delay of P_mP with respect to the extrapolation of the refraction from the 7.0 km/s layer and the rapid

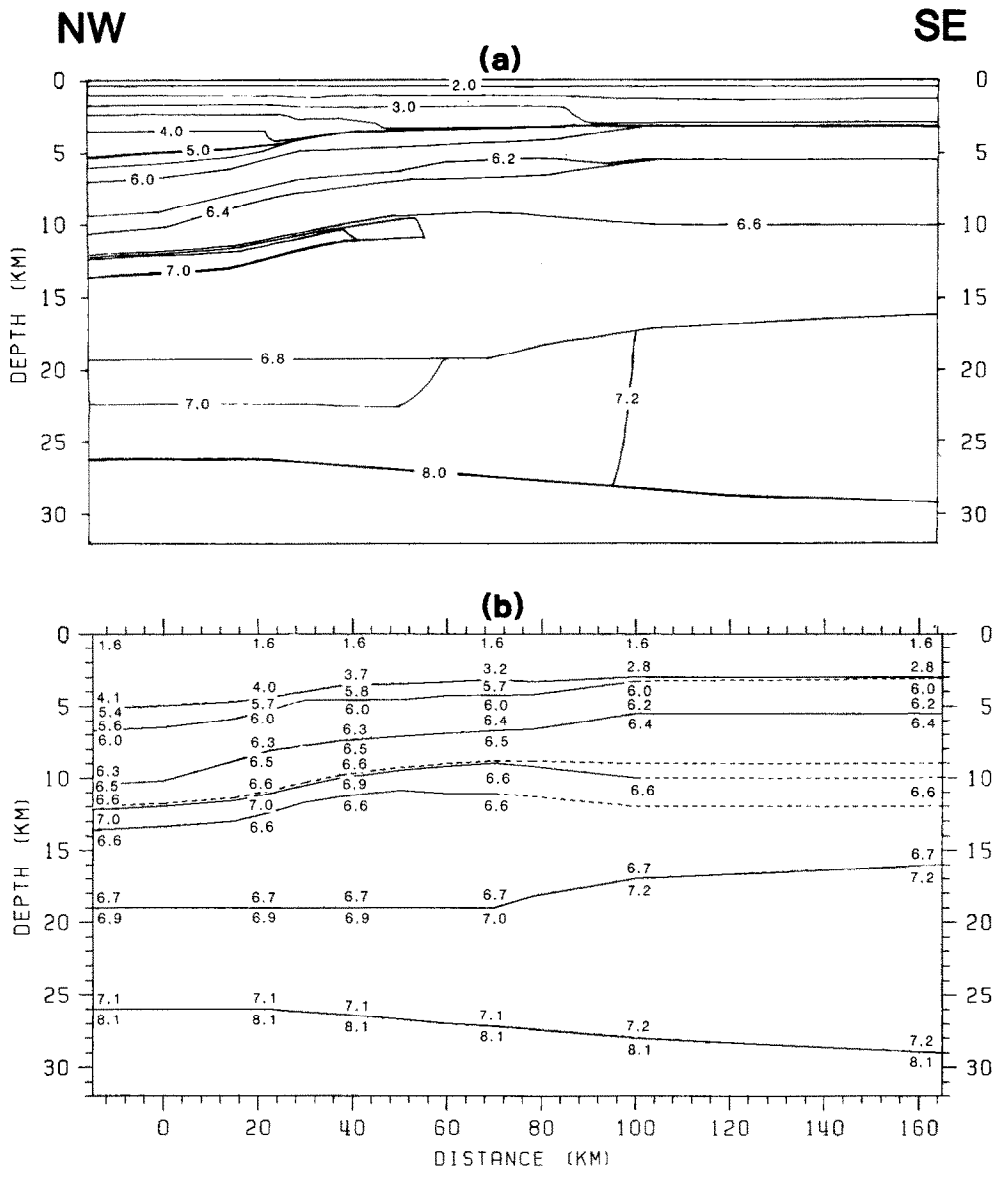

Fig. 7. Velocity model for central axial profile. a. Isovelocity lines, contoured at 0.5 km/s interval for velocity < 6.0 km/s and at 0.2 km/s interval for velocity > 6.0 km/s. b. Structural model.

amplitude decay of the 7.0 km/s refraction beyond 80 km range (*G*, Fig. 4). The velocity of this layer cannot be measured directly, but the location of the critical point from the reflection at the base of the LVL on SP14 (*H*, Fig. 4) is best matched for an LVL of velocity 6.6 km/s overlying a lower crust of velocity 7.0 km/s. If mid-crustal velocities are fairly continuous across the profile, further support for an LVL velocity of 6.6 km/s comes from the existence of mid-crustal velocities 6.6 km/s southeast of SP16. Here the mid-crust is no longer an LVL because the upper-crustal 7.0 km/s "lid" is absent, so that the mid-crustal velocity can be measured directly from first arrivals on SP15 (*F–G*, Fig. 5). A mid-crustal velocity of 6.6 km/s agrees with the velocity of 6.75 km/s determined at this depth by Colburn and Mooney (1986) on the parallel profile 10–15 km to the west.

Postcritical reflections from the base of the

mid-crust and from the Moho define a distinct lower-crustal unit whose thickness and velocity increase to the southeast. Critically-reflected arrivals from the mid-crust–lower crust boundary on SP14 (*H*, Fig. 5) require a lower-crustal velocity of 7.0 km/s in the center of the profile; for velocities lower than 7.0 km/s, no critical reflections would be generated beneath the upper-crustal 7.0 km/s lid. Furthermore, lower crustal velocities southeast of SP16 must be at least 7.2 km/s in order for the P_mP critical point, which is not observed on SP16-southeast, to lie beyond the end of the profile. The lack of a lower-crustal postcritical reflection on SP16-northwest indicates velocities lower than 7.0 km/s in the lower crust on the northwest side of the model; a velocity greater than 7.0 km/s at the top of the lower crust on the northwest would produce an observable critical reflection.

Crustal thickness varies along the model from 26 km in the northwest to 29 km in the southeast. The deeper Moho in the southeast is required, along with a lower-crustal velocity of at least 7.2 km/s, in order for the P_mP critical point to lie beyond the southeastern end of the profile on SP16. Because the crustal velocity structure is fairly well-constrained, this estimate of crustal thickness is probably accurate to ± 2 km. The upper mantle apparent velocity of 8.0 ± 0.1 km/s, observed on SP14 (*J*, Fig. 5), and the dip of the Moho suggest an upper mantle true velocity of 8.1 ± 0.1 km/s, consistent with Oppenheimer and Eaton (1984). The Moho relief of 3 km would create a Bouguer gravity anomaly of about 25 mGal, assuming a density contrast of 0.2 gm/cm^3 across the Moho. Actual Bouguer anomalies along this axial profile do not exceed 10–15 mGal; however, the negative Bouguer anomaly expected from the thicker sediments on the northwest side of the profile accounts for the difference. Detailed 2-D gravity modeling, especially in conjunction with interpretations of the cross-lines in the Great Valley refraction survey, will provide important constraints on final crustal models of the Great Valley.

We have computed 2-D synthetic seismograms for each shotpoint (Figs. 4–6) using the asymptotic ray theory and the method of McMechan and Mooney (1980). Synthetic modeling is particularly useful for discerning details which are indistinguishable on the basis of travel-time data alone, such as velocity gradients and velocity contrasts at interfaces. The synthetics show good first-order agreement with the observed data. In particular, the synthetic modeling helped adjust the velocity gradients in the sediments and basement in order to generate multiples with amplitudes comparable to first arrivals (for example, *AA* and *EE*, Fig. 4). The synthetics also point out the model's most striking shortcoming—the high-amplitude P_mP predicted at a range of only 75 km on SP15-southeast (Fig. 5). The observed P_mP on SP15-southeast first becomes prominent at a range of about 110 km. This discrepancy, as well as the rather erratic P_mP arrival times on SP14, reflects lateral complexity in the reflectivity and/or structure of the Moho which we have not attempted to model.

Discussion and conclusions

The geologic interpretation of seismic refraction results depends on the conversion of a velocity model into a petrological model. Caution must be exercised in this step, because there is no unique correspondence of P-wave velocity to rock type. Laboratory results in fact show a wide range of P-wave velocities for some rock types (e.g., Birch, 1960; Christensen, 1979). In order to reduce the ambiguity of our results, then, we will refer to existing geological models and other geophysical data from the Great Valley, particularly gravity, magnetic, and seismic reflection data. In this section, we discuss the possible composition of the crust of the Great Valley and address some of our model's implications on previous geological and geophysical work in the area.

Using relative P_n travel times of regional earthquakes, Oppenheimer and Eaton (1984) derived a contour map of crustal thickness for central California. Their contours predict a crustal thickness of 32 km beneath the axial profile, in contrast to our estimate of 27 km. The most likely reason for this discrepancy is that Oppenheimer and Eaton's data base requires that they show smooth, continuous contours between stations located in the

Coast Ranges and in the Sierra Nevada foothills, and therefore our crustal thickness estimate is a refinement of their earlier estimate. Oppenheimer and Eaton (1984) also presented evidence for a high-velocity lower crustal layer beneath the Great Valley based on a 7.4 km/s apparent velocity for an earthquake in the Sierra Nevada foothills recorded in the Coast Ranges. Our velocity model substantiates the presence of this high-velocity (7.0–7.2 km/s) basal crustal layer.

The crustal structure of the central Great Valley bears little similarity to the crustal structure of the adjacent Diablo Range (Walter and Mooney, 1982; Blümling and Prodehl, 1983). In the upper crust, at least, this is not surprising, since the Coast Ranges and Great Valley are distinct geologic provinces separated by a major tectonic boundary, the Coast Range (locally Ortigalita) fault. The dissimilarity even in the lower crust between our model and that of Blumling and Prodehl (1983), however, suggests that the Coast Ranges and Great Valley are separated by a fault or suture zone which extends throughout the crust. Furthermore, according to our model the crust under our profile is slightly thinner (26–29 km) than the crust under the Diablo Range (28–30 km, Walter and Mooney, 1982; 29–30 km, Blumling and Prodehl, 1983). This requires that the Moho rises slightly from the Diablo Range beneath the Great Valley before plunging beneath the Sierra Nevada to the east. Although Eaton (1966) suggested a thinning of the crust under the Great Valley, later models (e.g., Cady, 1975; Oppenheimer and Eaton, 1984) have depicted the crust as gradually thickening from the Diablo Range across the Great Valley.

Recent seismic reflection work near our profile has provided new evidence for complex basement tectonics in the Great Valley and Coast Ranges (Wentworth et al., 1984a, b; Zoback and Wentworth, 1985). Our refraction line crosses reflection line *CC-1* and passes just west of line *CC-2* (Fig. 1). From these and other reflection lines Wentworth et al. (1984a, b) inferred the existence of a wedge of Franciscan rocks thrust eastward over Great Valley basement, peeling up the overlying Great Valley sequence. The similarity in velocity between the Franciscan wedge (5.25–5.8 km/s) of Wentworth et al. (1984b) and our "hidden layer" (5.4–5.8 km/s) suggests they may be the same unit. This possibility is supported by the observation that the "hidden layer" is thickest on the northwest end of our profile, where the line bends toward the western side of the Great Valley, and disappears to the southeastern where the line lies along the central part of the Great Valley—consistent with the qualitative relation predicted by Wentworth et al.'s (1984b) cross-section along reflection profile *CC-1*.

Two observations, however, argue against the interpretation of the "hidden layer" as Franciscan rock. First, our profile crosses *CC-1* east of the projected easternmost tip of the Franciscan wedge, yet the "hidden layer" is still present there (km 59 of Fig. 4). Second, the few existing basement drill cores near the northwestern end of our line—which we used to define the top of the "hidden layer"—are annotated on drillers' logs as granite, presumably meaning crystalline rock, whereas the Franciscan assemblage consists mainly of graywacke and metagraywacke. Nevertheless, in view of the thinness of the "hidden layer" and the uncertainties in the exact location of the Franciscan wedge tip and in the petrology of the basement there, the possibility that the "hidden layer" is Franciscan rock cannot be ruled out.

One crucial question which must be addressed by our interpretation is whether the velocity structure of the upper crust beneath the Great Valley sediments is more indicative of oceanic crust or continental crust. According to one tectonic model, the basement of the western Great Valley was originally oceanic crust created by backarc spreading above a westward-subducting slab behind a Jurassic island arc located west of the young Sierra Nevada. During the Late Jurassic Nevadan orogeny, this island arc collided with the Sierra Nevada arc massif, creating the Foothills Suture Zone (Schweikert and Cowan, 1975). Eastward subduction of the Farallon Plate beneath the North American Plate then began at the Coast Ranges subduction zone, creating a forearc basin between the Franciscan subduction complex and the Sierra Nevada island arc. The latest-Jurassic to Cretaceous Great Valley sequence was deposited in this forearc basin, on top of the remnant backarc

oceanic crust (Fig. 8; Dickinson, 1981). The contact between the oceanic and island arc crust is presumably buried beneath the Great Valley sedimentary section and may be marked by the steep eastern gradient of the prominent Great Valley magnetic anomaly (Griscom, 1982). If this model is correct, our profile, which lies west of the magnetic anomaly gradient (Fig. 1), should overlie oceanic crust.

We tested this hypothesis by comparing a velocity–depth function of the upper crust from the northwest end of our model to velocity–depth functions determined in oceanic crust older than 20 m.y. (Spudich and Orcutt, 1980). This comparison (Fig. 9) shows that the upper crust beneath this portion of the central Great Valley has a thickness and velocity structure compatible with *in situ* oceanic crust. The match is not perfect: our 6.5–6.6 km/s layer is slower than the corresponding oceanic crust (6.8–7.0 km/s), and the "hidden layer" (5.4–5.7 km/s) is faster than its oceanic counterpart (< 5.0 km/s). The velocity of the 7.0 km/s layer agrees well with that of the lower crust in the ocean and is probably a gabbroic fragment of oceanic crust, or possibly serpentinized peridotite. Velocities measured in the Point Sal ophiolite (Nichols et al., 1980) are also comparable to the Great Valley basement velocities (layers of 4.9–5.4, 6.0, 6.0–7.0, and 7.1 km/s), although the ophiolite there is thinner (3 km), and the 6.0 km/s layer is almost absent. We interpret the upper 7–8 km of the basement beneath the northwest end of our profile as ophiolite, which we will refer to as the "central line ophiolite." This ophiolite is probably not continuous along the length of our profile, as the upper-crustal 7.0 km/s, which we regard as diagnostic of the ophiolite, disappears to the southeast.

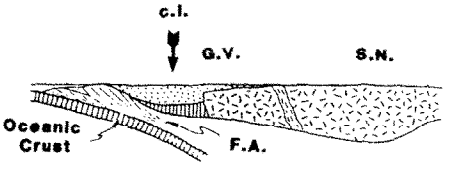

Fig. 8. Model of the northern California Cenozoic (pre-San Andreas) forearc region, adapted from Dickinson (1981). Great Valley (*G.V.*) sediments were deposited in forearc basin on remnant backarc oceanic crust. *S. N.*—Sierra Nevada, *F.A.*—Franciscan assemblage, *c.l.*—central refraction line.

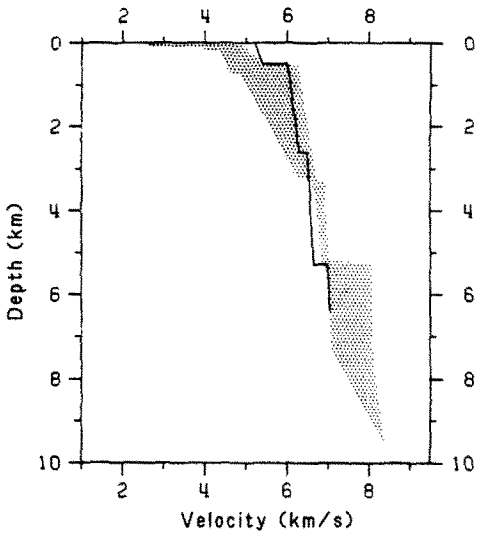

Fig. 9. Model velocity–depth function for the upper crust (bold line) at model km 30 compared to range of velocity–depth functions (shaded region) in oceanic crust from marine refraction surveys in crust older than 20 m.y. (from Spudich and Orcutt, 1980).

Comparison of our velocity–depth function to that of the western axial profile 10–15 km to the west (Fig. 10) shows that the central line ophiolite is also discontinuous across the axis of the Great Valley. The upper-crustal 7.0 km/s layer is absent beneath the western profile (Colburn and Mooney, 1986). Instead, the upper and mid-crust there comprise two layers with average velocities of 6.1 and 6.75 km/s and thicknesses of 5 and 6 km, respectively. Colburn and Mooney (1986) compare this velocity structure with the 6.2 and 6.6 km/s layers found beneath the metamorphic and igneous rocks of the Sierra Nevada foothills by Spieth et al. (1981). The absence of a velocity–depth structure appropriate for ophiolite beneath the western axial line indicates that, unless it is too thin to be resolved by seismic refraction, the Coast Range ophiolite, which underlies the Great Valley sequence in outcrops in the eastern Coast Ranges (Fig. 1), does *not* continue eastward beneath the valley to connect with either the central line ophiolite or the Smartville ophiolite of the Sierra Nevada. The eastward extent of the central

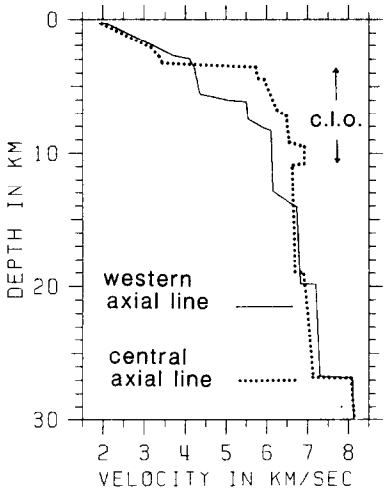

Fig. 10. Comparison of velocity–depth functions from the central axial refraction line (our model, km 30) and the western axial line (Colburn and Mooney, 1986). The high-velocity basement of the central line is called the central line ophiolite (*c.l.o.*).

line ophiolite is unconstrained by the present refraction survey, since neither the cross-lines (Whitman et al., 1985) nor the eastern axial profile (Fig. 1) provide resolution of velocities below the upper crust. The central line ophiolite, if viewed in outcrop pattern on the surface of the Great Valley basement, may form a long, string-like slice of ophiolite similar in pattern to the Coast Range and Smartville ophiolites exposed on either side of the valley. Spieth et al. (1981) also found a discontinuous, 7.0 km/s layer (at 5 km depth), suggesting that fragments of ultramafic rocks embedded in igneous amd metamorphic island-arc rocks may be fairly common beneath the Sierra Nevada foothills and the Great Valley.

The prominent Great Valley magnetic and gravity anomalies, the peaks of which lie about 10 km east of our profile (Fig. 1), should provide some clues about the geometry of the central line ophiolite. In order to fit gravity, magnetic, and limited seismic refraction data, Cady (1975) modeled the crust beneath the Great Valley sediments as a dense (2.98 g/cm^3), high-velocity (6.8 km/s) layer with a thickness of 25–30 km. Our data, which are much more detailed than the seismic data available to Cady (1975), show significantly lower velocities in the upper crust. The Great Valley magnetic and gravity anomalies must therefore be caused by something other than Cady's postulated dense, high-velocity basement directly beneath the sedimentary column. Griscom and Jachens (1986) interpreted the Great Valley magnetic and gravity anomalies 100 km south of our study area (along reflection line SJ-19, Wentworth et al., 1984a) as arising from a suture zone between mafic basement to the west and silicic basement to the east. The discovery of the central line ophiolite qualitatively supports the idea that mafic or ultramafic rocks beneath the Great Valley are responsible for the magnetic and gravity anomalies. However, the lateral discontinuity of the ophiolite suggests that the source of the anomalies is more complicated than a simple oceanic–continental contact. A more detailed determination of the geometry of the body responsible for the Great Valley anomalies will have to await further gravity and magnetic modeling based on the refraction and reflection data.

The middle and lower crust in the central Great Valley are probably mafic rocks, perhaps of intermediate or high metamorphic grade. The mid-crust (6.6–6.7 km/s) has a velocity compatible with gabbro (Lin and Wang, 1980), granulite, or amphibolite (Christensen, 1979); mixtures of diorite with these rock types are also possible compositions for the mid-crust. The lower crust (7.0–7.2 km/s) has a velocity compatible with gabbro (Birch, 1960; Christensen, 1979) or amphibolite (Christensen, 1965). In view of the geologic history of California, involving active subduction of oceanic crust and island arc plutonism, it is likely that the middle and lower crust of the Great Valley consist of basaltic rock emplaced by magmatic or tectonic underplating, or both. Magmatic underplating could have resulted from asthenospheric upwelling through the triangular slab window created by the progressive replacement of the California subduction zone by the San Andreas transform margin since the Oligocene (Dickinson and Snyder, 1979). Lithospheric upwelling and accretion beneath an originally thin (20 km) Coast Range crust has been modeled as the cause of the Coast Range heat flow anomaly south of the Mendocino triple junction (Lachenbruch and Sass, 1980). Tectonic un-

derplating could have resulted from periodic incorporation into the lower crust of oceanic crust and/or accretionary complex rocks above the subducting lithospheric slab during the late Mesozoic and early Tertiary, as has been proposed for the Mesozoic subduction complex in southern Alaska (Page et al., 1986).

In conclusion, the crust of the central Great Valley comprises a 3–5 km thick sedimentary section, a four-layer basement with velocities increasing from 5.4 to 7.0 km/s, a mid-crust of 6.6 km/s, and a lower crust of 6.9 to 7.2 km/s. The upper basement on the northwestern part of the model has a thickness and velocity structure compatible with oceanic crust, and we interpret it as a fragment of ophiolite. This ophiolite does not continue as far as the western axial refraction profile 10–15 km to the west, and its eastern extent is unknown. Gravity and magnetic modeling should help determine its geometry. The middle and lower crust are probably gabbroic and the result of tectonic or magmatic underplating, or both. The dissimilarity in crustal structure between the Diablo Range and Great Valley suggests that a fault or suture zone separates these provinces throughout the crust. Crustal thickness varies from 26 to 29 km along our profile, indicating that the Moho rises slightly from the Diablo Range to Great Valley before plunging beneath the Sierra Nevada to the east.

Acknowledgments

This study is the result of the cooperation and contributions of many people. For their efforts in the field we thank A. Bokun, J.M. Bonomolo, E.E. Criley, K.E. Harrington, L.R. Hoffman, R.P. Meyer Jr., G.A. Molina, J.M. Murphy, J.R. VanShaack, and V.D. Sutton. We thank J.H. Luetgert for raytracing and synthetic seismogram software support. The ideas and constructive criticism of A.W. Walter, C.M. Wentworth, R.H. Colburn, D. Whitman, A. Griscom, R. Jachens, E. Ambos, J.H. Luetgert, L.J. Hwang, and R.D. Catchings were invaluable. Thoughtful reviews by M.C. Blake, J.P. Eaton, L. Braile, and K. Ito much improved the manuscript.

References

Bartow, J.A., 1983. Map showing configuration of the basement surface, northern San Joaquin Valley, California. U.S. Geol. Surv., Misc. Field Studies Map MF-1430, 1:250,000.

Birch, F., 1960. The velocity of compressional waves in rocks to 10 kilobars, Part 1. J. Geophys. Res., 65: 1083–1102.

Blake, M.C., Jayko, A.S. and McLaughlin, R., 1984. Tectonostratigraphic terranes of the northern Coast Ranges, California. In: Tectonostratigraphic Terranes of the Circumpacific Region. Circumpac. Counc. Ener. Miner. Resour., Earth Sci. Ser., 1: 1984.

Blümling, P. and Prodehl, C., 1983. Crustal structure beneath the eastern part of the Coast Ranges (Diablo Range) of central California from explosion seismic and near earthquake studies. Phys. Earth Planet. Inter., 31: 313–326.

Cady, J.W., 1975. Magnetic and gravity anomalies in the Great Valley and western Sierra Nevada metamorphic belt, California Province. Geol. Soc. Am., Spec. Pap., 186: 56 pp.

Červený, V., Molotkov, I.A. and Pšenčík, I., 1977. Ray Method in Seismology. Univ. of Karlova, Prague, 214 pp.

Christensen, N.I., 1979. Compressional wave velocity in rocks at high temperatures and pressures, critical thermal gradients, and crustal low-velocity. J. Geophys. Res., 84: 6849–6857.

Colburn, R.H. and Mooney, W.D., 1986. Two-dimensional velocity structure along the synclinal axis of the Great Valley, California. Bull. Seismol. Soc. Am., 75: 175–191.

Day, H.W., Moores, E.M. and Tuminas, A.C., 1985. Structure and tectonics of the northern Sierra Nevada. Geol. Soc. Am. Bull., 96: 436–450.

Dickinson, W.R., 1981. Plate tectonics and the continental margin of California. In: W.G. Ernst (Editor), The Geotectonic Development of California (Rubey Volume I). Prentice-Hall, Englewood Cliffs, N.J., pp. 1–28.

Dickinson, W.R. and Snyder, W.S., 1979. Geometry of subducted slabs related to San Andreas transform. J. Geol., 87: 609–627.

Eaton, J.P., 1963. Crustal structure from San Francisco, California, to Eureka, Nevada, from seismic refraction measurements. J. Geophys. Res., 68: 5789–5806.

Eaton, J.P., 1966. Crustal structure in northern and central California from seismic evidence. In: E.H. Bailey (Editor), Geology of Northern California. Calif. Div. Mines Geol. Bull., 190: pp. 419–426.

Griscom, A., 1982. Magnetic interpretation of ophiolites and batholiths in California. Geol. Soc. Am. Abstr. Progr., 14.

Griscom, A. and Jachens, R.C., 1986. Tectonic implications of gravity and magnetic models along east-west seismic profiles near Coalinga, California. In: M.J. Rymer and W. Ellsworth (Editors), Mechanics of the Coalinga, California Earthquake. U.S. Geol. Surv., Prof. Pap., in press.

Healy, J.H., Mooney, W.D., Blank, H.R., Gettings, M.E., Kohler, W.M., Lamson, R.J. and Leone, L.E., 1982. Saudi Arabian seismic deep-refraction profile: final project report. U.S. Geol. Surv., Saudi Arabian Mission Rep. 02-37, 429 pp.

Lachenbruch, A.H. and Sass, J.H., 1980. Heat flow and energetics of the San Andreas fault zone. J. Geophys. Res., 85: 6185–6222.

Lin, W. and Wang, C.Y., 1980. P-wave velocities in rocks at high pressure and temperature and the constitution of the central California crust. Geophys. J.R. Astron. Soc., 61: 379–400.

McMechan, G.A. and Mooney, W.D., 1980. Asymptotic ray theory and synthetic seismograms for laterally varying structures: theory and application to the Imperial Valley, California. Bull. Seismol. Soc. Am., 70: 2021–2035.

Nichols, J., Warren, N., Luyendyk, B.P. and Spudich, P., 1980. Seismic velocity structure of the ophiolite at Point Sal, southern California, determined from laboratory measurements. Geophys. J.R. Astron. Soc., 63: 165–185.

Oppenheimer, D.H. and Eaton, J.P., 1984. Moho orientation beneath Central California from regional earthquake travel times. J. Geophys. Res., 89: 10,267–10,282.

Page, R.A., Plafker, G., Fuis, G.S., Nokleberg, W.J., Ambos, E.L., Mooney, W.D. and Campbell, D.L., 1986. Accretion and subduction tectonics in the Chugach Mountains and Copper River Basin, Alaska: initial results of the Trans-Alaska Crustal Transect. Geology, 14: 501–505.

Schweikert, R.A. and Cowan, D.S., 1975. Early Mesozoic tectonic evolution of the western Sierra Nevada, California. Geol. Soc. Am. Bull., 86: 1329–1336.

Spieth, M.A., Hill, D.P. and Geller, R.J., 1981. Crustal structure in the northwestern Foothills of the Sierra Nevada from seismic refraction experiments. Bull. Seismol. Soc. Am., 71: 1075–1087.

Spudich, P. and Orcutt, J., 1980. A new look at the seismic velocity structure of the oceanic crust. Rev. Geophys. Space Phys., 18: 627–645.

Walter, A.W. and Mooney, W.D., 1982. Crustal structure of the Diablo and Gabilan Ranges, Central California: a reinterpretation of existing data. Bull. Seismol. Soc. Am., 72: 1567–1590.

Wentworth, C.M., Zoback, M.D. and Bartow, J.A., 1984a. Tectonic setting of the 1983 Coalinga earthquake from seismic reflection profiles: a progress report. U.S. Geol. Surv., Open-File Rep., 85-44: 19–30.

Wentworth, C.M., Blake, M.C., Jr., Jones, D.C., Walter, A.W. and Zoback, M.D., 1984b. Tectonic wedging associated with emplacement of the Franciscan assemblage, California Coast Ranges. Soc. Econ. Petrol. Mineral., Pac. Sec., 43: 163–173.

Whitman, D., Walter, A.W. and Mooney, W.D., 1985. Crustal structure of the Great Valley, California: cross profile. Eos, Trans. Am. Geophys. Union, 66 (abstr.).

Zoback, M.D. and Wentworth, C.M., 1986. Crustal studies in Central California using an 800-channel seismic reflection recording system. In: M. Barazangi and L. Brown (Editors), Reflection Seismology: A Global Perspective. Am. Geophys. Union, Geodyn. Ser., 13.